ORIGINAL ARTICLE

The Glutamine Transporter Slc38a1 Regulates GABAergic Neurotransmission and Synaptic Plasticity

Tayyaba Qureshi[1], Christina Sørensen[2,3], Paul Berghuis[4], Vidar Jensen[1], Marton B. Dobszay[4], Tamás Farkas[4], Knut Tomas Dalen[5], Caiying Guo[6], Bjørnar Hassel[7], Tor Paaske Utheim[8,9], Øivind Hvalby[1], Torkel Hafting[1], Tibor Harkany[4,10], Marianne Fyhn[2] and Farrukh Abbas Chaudhry[1,9]

[1]Department of Molecular Medicine, University of Oslo (UiO), Oslo, Norway, [2]Department of Biosciences, UiO, Oslo, Norway, [3]Department of Neuroscience, University of Copenhagen, Copenhagen, Denmark, [4]Department of Neuroscience, Karolinska Institutet, Stockholm, Sweden, [5]Department of Nutrition, UiO, Oslo, Norway, [6]Janelia Research Campus, Ashburn, Virginia 20147, USA, [7]Department of Neurohabilitation, Oslo University Hospital (OUH) and UiO, Norway, [8]Department of Medical Biochemistry, OUH, Norway, [9]Department of Plastic and Reconstructive Surgery, OUS and UiO, Norway and [10]Department of Molecular Neurosciences, Center for Brain Research, Medical University of Vienna, Austria

Address correspondence to email: f.a.chaudhry@medisin.uio.no

Øivind Hvalby passed away 23rd May 2015

Abstract

GABA signaling sustains fundamental brain functions, from nervous system development to the synchronization of population activity and synaptic plasticity. Despite these pivotal features, molecular determinants underscoring the rapid and cell-autonomous replenishment of the vesicular neurotransmitter GABA and its impact on synaptic plasticity remain elusive. Here, we show that genetic disruption of the glutamine transporter Slc38a1 in mice hampers GABA synthesis, modifies synaptic vesicle morphology in GABAergic presynapses and impairs critical period plasticity. We demonstrate that Slc38a1-mediated glutamine transport regulates vesicular GABA content, induces high-frequency membrane oscillations and shapes cortical processing and plasticity. Taken together, this work shows that Slc38a1 is not merely a transporter accumulating glutamine for metabolic purposes, but a key component regulating several neuronal functions.

Key words: GABA, neurotransmitter replenishment, SAT1, Slc38, SNAT1

Introduction

GABA is the principal inhibitory neurotransmitter in the central nervous system (CNS) with manifold functions: it regulates action potential (AP) firing and network synchrony through perisomatic inhibition and the efficacy and plasticity of excitation by dendritic inhibition (Klausberger and Somogyi 2008; Huang 2009; Hu et al. 2014). GABA signaling can be either short-lived and phasic when GABA is released *in quanta* to act at synaptic GABA$_A$ receptors or long-lasting and tonic upon ambient extracellular GABA stimulating extra-synaptic receptors (Isaacson

and Scanziani 2011). In addition, GABA affects developmentally coded cortical critical period plasticity by modulating interneuron migration, placement and synaptic wiring (Ben-Ari et al. 2007). Indeed, at the systems level, GABA signaling underpins learning, memory, cognition and sensory perception (Buzsaki et al. 2007). The life-long competence of GABA signaling relies on efficient local means for neurotransmitter reuptake, replenishment and release. Considering the prominence of dysfunctional GABA signaling in brain disorders, such as epilepsy, autism, schizophrenia and anxiety (Soghomonian and Martin 1998; Lewis et al. 2012), it is surprising that molecular determinants rate-limiting precursor availability for metabolic replenishment and vesicular filling and their impact on inhibitory synaptic plasticity remain elusive.

To describe precursor replenishment, the "glutamate/GABA-glutamine (GGG) cycle" was proposed decades ago, which suggests that GABA (and glutamate) upon transport into perisynaptic astroglia is first converted into glutamine, which is then transported back into neurons to regenerate GABA as neurotransmitter (Reubi et al. 1978; Nissen-Meyer and Chaudhry 2013). This is supported by elucidation of the unconventional kinetics combined with the cell-specific localization of a family of amino acid (AA) transporters

(Slc38) (Nissen-Meyer and Chaudhry 2013): system N transporters Slc38a3 (SN1/SNAT3) and Slc38a5 (SN2/SNAT5) reside on astroglial membranes and work bi-directionally to supply neurons with glutamine (Chaudhry et al. 1999; Hamdani et al. 2012). Heterologous expression of the homologous system A transporter (SAT) Slc38a1 (SAT1/SNAT1/SA2) in cultured mammalian cells shows transport of amino acids with a preference for glutamine (Varoqui et al. 2000; Chaudhry et al. 2002). We have shown that Slc38a1 is enriched in GABAergic neurons and based on this localization proposed that Slc38a1 could be involved in the replenishment of the neurotransmitter GABA (Solbu et al. 2010). However, this has been contested by a number of papers reporting that Slc38a1 occurs indiscriminately in glutamatergic, GABAergic, cholinergic and dopaminergic neurons and targeted primarily to their somatodendritic compartments implicating a broader role in general cellular metabolism (Mackenzie et al. 2003; Conti and Melone 2006). In addition, the functional significance of glutamine in GABA replenishment and the existence of a GGG cycle remain ambiguous since some studies have shown unchanged neurotransmission upon pharmacological inhibition of system A transporters, inactivation of phosphate-activated glutaminase (PAG) and/or removal of
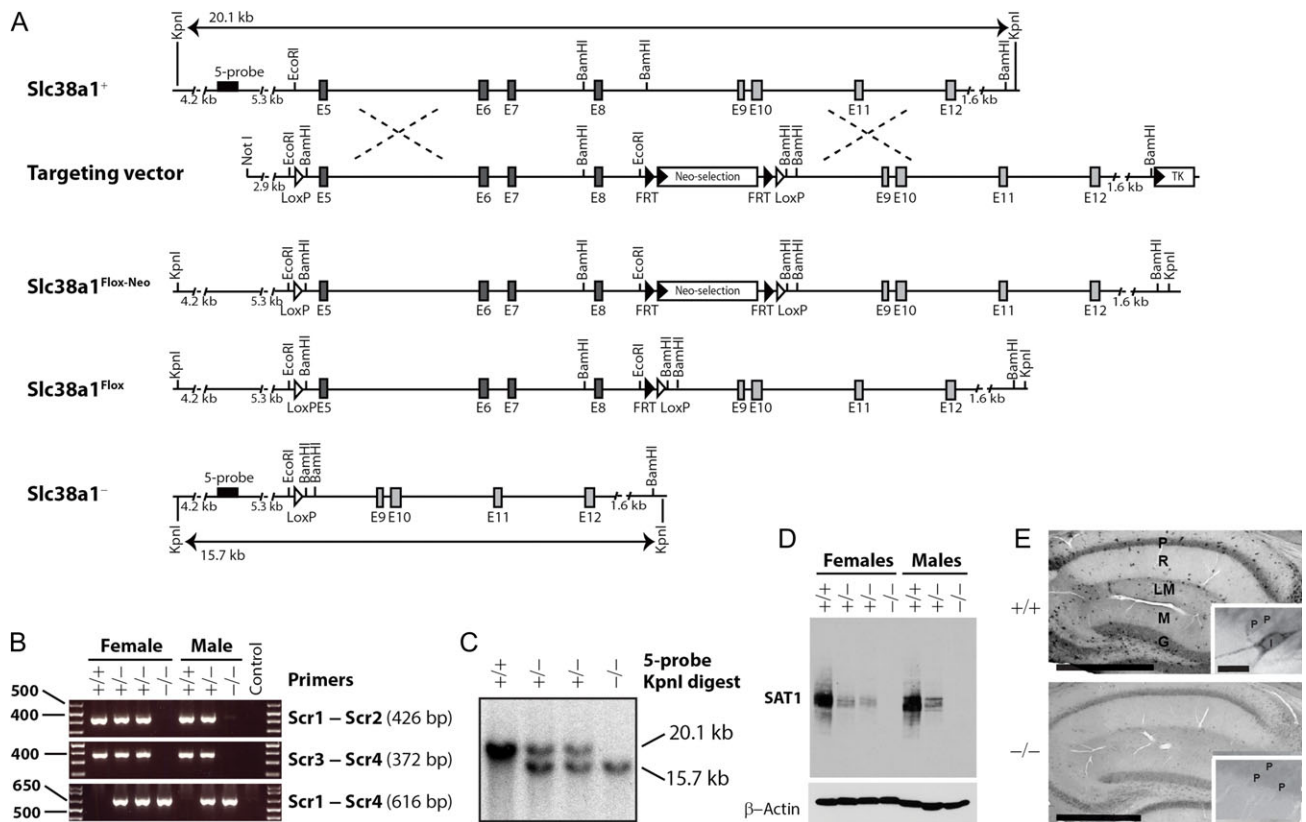
Figure 1. Genetic inactivation of Slc38a1 using the binary Cre/LoxP system and its validation. (A) Schematic drawing of the targeting vector, wild-type allele (Slc38a1^{wt} (Slc38a1$^+$)), and targeted alleles (Slc38a1$^{flox-Neo}$, Slc38a1^{flox}, and Slc38a1^{null} (Slc38a1$^-$)). The Slc38a1 targeting vector contained a LoxP site (inserted into intron 4; white triangles), and a selection cassette (Neomycin) flanked by FRT-sites (black triangles) and a LoxP site (inserted into intron 8). After homologous recombination in ES cells (Slc38a1$^{flox-Neo}$ locus), ES cells were transected with Flp to excise the selection cassette (Slc38a1^{flox} locus) prior to blastocyst injection. Upon expression of Cre recombinase, exons 5–8 were excised (Slc38a1 null), generating out of reading frame splicing transcript. The binding site for the 5-end Southern screening probe and the expected fragment sizes after KpnI digest are indicated. (B) Genotyping of ear biopsies of Slc38a1$^{+/+}$, Slc38a1$^{+/-}$ (heterozygous) and Slc38a1$^{-/-}$ mice by 3 pairs of probes gives the expected amplified fragments (see Supplementary Experimental Procedures). (C) Southern blot analysis of DNA isolated from liver of Slc38a1$^{+/+}$, Slc38a1$^{+/-}$, and Slc38a1$^{-/-}$ mice. DNA was digested with KpnI followed by hybridization with the 5-probe to give the expected fragments for Slc38a1^{WT} (20.2 kb) and Slc38a1^{Null} (15.7 kb). (D) Expression of Slc38a1 protein in brain lysates of Slc38a1$^{+/+}$, Slc38a1$^{+/-}$, and Slc38a1$^{-/-}$ mice was investigated. No protein expression is detected in lysates from Slc38a1$^{-/-}$ mice, while Slc38a1$^{+/-}$ mice show reduced staining for Slc38a1 protein compared to Slc38a1$^{+/+}$ mice. β-actin was used as loading control. E) Expression of Slc38a1 protein was investigated by immunostaining of free-floating brain sections for Slc38a1. In the hippocampus, Slc38a1 immunoreactivity accumulates in scattered interneuron-like cells in the CA1 and dentate area of Slc38a1$^{+/+}$ mice. Such staining is abolished in sections from Slc38a1$^{-/-}$ mice. G, granular; LM, lacunosum-moleculare; M, moleculare; P, pyramidale; R, Radiatum. Insets: P, pyramidal cells; I, interneuron-like cell. Scale: 100 μm.

external glutamine (Masson et al. 2006; Kam and Nicoll 2007). Thus, conclusive experimental evidence for the function of Slc38a1 *in vivo* and its impact on inhibitory synaptic plasticity, and the molecular determinants of GABA replenishment and GABAergic vesicular load are lacking, and more broadly, for the existence of a GGG cycle.

Here, we have genetically inactivated Slc38a1 in mice and characterized their phenotype at successive levels of cellular and network complexity *in vitro* and *in vivo*. We demonstrate that Slc38a1 sustains replenishment of GABA, impacts vesicle morphology and neurotransmitter content, triggers AP generation and regulates inhibitory synaptic plasticity *in vivo*.

Materials and Methods

Animal Handling

Experiments were approved and conducted in accordance with the Norwegian Animal Welfare Act and the European Convention for the Protection of Vertebrate Animals used for Experimental and Other Scientific Purposes (ETS 123). The mice were kept and handled under veterinary supervision at the UiO. Mice were housed in a temperature controlled facility (22–26 °C) with 50 ± 10% humidity and a 12-hours light/dark cycle. Animals were served municipal water and fed ad libitum with RM3 (E) from Special Diets Services (UK).

Discharge/frequency experiments on animals were performed at Karolinska Institutet and conformed to the European Communities Council Directive (86/609/EEC) and were approved by the Stockholms Norra Djurförsöksetiska Nämnd (N26/2005 and N38/2005).

Generation of a floxed Slc38a1 Mouse

The floxed Slc38a1 targeting construct was produced (Fig. 1A) using recombineering techniques (Liu et al. 2003). A 12 904 bp genomic DNA fragment containing exons 5–12 of the Slc38a1 gene was retrieved from BAC clone RP23-85D13. A LoxP sequence was inserted in intron 4 and a FRT-PGKNeo-FRT-LoxP cassette was inserted in intron 8. Thus, a fragment of 4504 bp genomic DNA containing exons 5 through 8 was floxed. Cre excision would generate an out-of-frame deletion. The targeting vector was electroporated into D1 embryonic stem (ES) cells which were derived from F1 hybrid blastocyst of 129S6 × C57BL/6 J. G418 resistant ES colonies were isolated and screened by nested polymerase chain reaction (PCR) using primers outside the construct paired with primers inside the neo cassette. Fourteen clones PCR positive for both arms were identified from 48 clones screened. Chimeric mice were generated by aggregating the ES cells with 8-cell embryos of CD-1 strain. The neo cassette was removed by mating the chimeras with 129S4/SvJaeSor-Gt(ROSA)26Sor$^{tm1(FLP1)Dym}$/J (Stock number: 003946) homozygous females. The F1 pups were genotyped by PCR using primers flanking LoxP or FRT-LoxP sites. The mice were then crossed with Deleter mice to create a systemic deletion of Slc38a1 (Schwenk et al. 1995). As Slc38a1 expression is restricted to some few organs (Chaudhry et al. 2002), secondary effects on the CNS phenotype is not very likely. Null mutant (Slc38a1$^{-/-}$) mice did not carry any obvious phenotypic abnormalities. We had several breedings (het x het, ko x ko, wt x wt) and all were backcrossed between 5 and 10 times. In addition, the mice were crossed with wt mice regularly in order to avoid inbreeding of the mice in order to reduce the risk of differences in the genetic background.

A new set of primers were designed for PCR genotyping. The template DNA was obtained by digesting an ear piece using the REDExtract-N-Amp™ Tissue PCR Kit (Sigma) followed by PCR-amplification of 1 μl of the template in a 10 μl PCR reaction. The reaction was carried out for 35 cycles (94 °C 30 s, 60 °C 30 s and 72 °C 30 s) followed by one cycle of 72 °C for 10 min.

Primers Used for Generation of a Floxed Slc38a1 Mice and for Investigating Their Genotypes

The homologous arms were 2945 bp (5′) and 5440 bp (3′). Primer sequences for ES screening were: 5′ arm forward primers: Slc38a1 Scr F1 (5′- cgtgttctccgtcagctatt-3′) and Slc38a1 Scr F2 (5′- atgtccggcagagtctttga-3′). Reverse primers: LoxP Scr R1 (5′-gagggacctaataacttcgt-3′) and LoxP Scr R2 (5′-ggaattgggctgcaggaatt-3′). 3′ arm forward primers: FRT Scr F1 (5′-ttctgaggcggaaagaacca-3′) and FRT Scr F2 (5′-cgaagttattaggtggatcc-3′); Reverse primers: Slc38a1 Scr R1 (5′-agtgatggtaaccgtcctgt-3′) and Slc38a1 Scr R2 (5′-ctactggccaggaacaacgat-3′).

A new set of primers were designed for PCR genotyping. The primer combination Scl38a1-Scr1: (5′-tgtaggtctgttcccatgttgtcct-3′) and Scl38a1-Scr2: (5′-gatgaaatgttccccggagtctaac-3′) generates a PCR product of 426 bp for the wild type allele, and 514 bp for the floxed allele. The primer set Scl38a1-scr3 (5′-tctcccactaagttgcgttgtcttc-3′) and Scl38a1-scr4(5′-ccaaatggatgacttggagattgtc-3′) generates a PCR product of 372 bp for the wild type allele and 471 bp for the floxed allele. Detection of the null allele after Cre excision was detected using the primer combination Scl38a1-Scr1 and Scl38a1-Scr4 giving a PCR product of 616 bp for the null allele and a fragment too large to be amplified for the wild type allele.

Southern Blotting

The probe sequence was radiolabelled with [a-32P]dCTP (Perkin Elmer, Wellesley, MA) using Megaprime DNA labelling System (Amersham Biosciences) prior to hybridization of the membrane to verify homologous recombination of the loci in the animals.

Synaptosomes, Amino Acid Analysis, and Quantitative Western Blotting

Synaptosomes were made by homogenization of the brains in ice cold 0.32 M sucrose 5% (w/v) followed by several steps of ultracentrifugation, as described (Bogen et al. 2006). Synaptosomal amino acids were separated and quantified by HPLC and fluorescence detection after pre-column derivatization with o-phthaldialdehyde (Hassel and Brathe 2000). Western blot analyses were performed as described (Nissen-Meyer et al. 2011). For details, see SI.

Light- and Electron Microscopic Cytochemistry

Ten pairs of age- and sex-matched Slc38a1$^{+/+}$ and Slc38a1$^{-/-}$ mice were deeply anesthetized with intra-peritoneal injection of Zoletil-mix 125 mg/kg. Five of the pairs were fixed by trans-cardiac perfusion of 4% paraformaldehyde (PFA) for immune-peroxidase staining and 5 pairs were perfusion fixed with 4% PFA and 2.5% glutaraldehyde (GA), hippocampal CA1 regions dissected out, embedded in Durcupan (FLUKA), sectioned (~100 nm), immunogold labeled and analyzed by Electron microscopy, as described (SI; Jenstad et al. 2009; Solbu et al. 2010).

Antibodies

Antibodies were generated against the most divergent and antigenic regions of the members of the Slc38 family of amino acid/glutamine transporters, Slc17 family of vesicular glutamate transporters and Slc32 family of vesicular GABA transporter by subcloning these sequences C-terminal to the sequence for glutathione-S-transferase (GST), inducing the protein in Escherichia coli and immunizing 2–6 rabbits for each protein. The antiserum obtained has been vigorously affinity purified by absorbing against immobilized GST followed by isolating on a column with immobilized GST-fusion protein containing the antigenic peptide used to immunize rabbits. These antibodies have then been properly characterized in our previous publications (e.g., Chaudhry et al. 1998; Boulland et al. 2003; Boulland et al. 2004; Jenstad et al. 2009; Solbu et al. 2010; Hamdani et al. 2012). Antibodies against AAs were generated by conjugating Bovine Serum Albumin (BSA) to the AAs by glutaraldehyde. The BSA-conjugates were separated by dialysis and mixed with adjuvant and injected intracutaneously in rabbits. Please, see detailed information on the procedure (Ottersen and Storm-Mathisen 1984) and the characterization of some of the antibodies in our previous publications (Jenstad et al. 2009; Solbu et al. 2010). Commercial antibodies against other proteins were used according to recommendations from the companies. Goat anti-rabbit and anti-mouse IgG Horseradish Peroxidase for western blotting (Thermo Fischer Scientific) and the biotin-streptavidin-peroxidase system and DAB were used as described earlier (Jenstad et al. 2009; Solbu et al. 2010). Commercial antibodies against other proteins were only used if they showed right band on western blots and had been characterized and published elsewhere. They were used according to recommendations from the companies.

Extracellular Recordings

Extracellular recordings were performed on 400 μm thick hippocampal slices prepared from adult (>P60) from Slc38a1$^{+/+}$ and Slc38a1$^{-/-}$ mice. Data are presented as mean ± S.E.M. Statistical significance was evaluated by using a linear mixed model analysis (SAS 9.1), with $P < 0.05$ being designated as statistically significant. See SI for details.

Interneuron studies

Isolation of interneurons and their analyses were performed according to (Berghuis et al. 2004). For details, see SI.

Monocular Deprivation and In vivo Electrophysiology

Extracellular recordings of single unit activity and local field potentials were made using linear silicone probes with 16 recording sites spaced at 50 μm intervals (NeuroNexus probes, A1x16-3 mm-50-177). Craniotomies to expose the primary visual cortex (2 mm in diameter, 1 mm anterior and 3 mm lateral to lambda) were made above one (contralateral to the deprived eye in MD animals or both hemispheres (control animals). The electrode was lowered into the brain to a depth of 1000 μm in the V1B, and was allowed to settle for 20 min before recording. Electrophysiological recordings were performed under light isoflurane anesthesia (0.5–1%) supplemented with intramuscular administration of chlorprothixene (0.2 mg). Visual stimuli was generated using Psychophysics Toolbox extension (Brainard 1997) for MATLAB (Mathworks) and sinusiodal drifting gratings were displayed on a 21" computer monitor centered 25 cm in front of the animal. Four days of MD was started between postnatal day 25 (P25) and P27. Eyelids were sutured shut under isoflurane anesthesia.

Statistical Analysis

All values are presented as mean ± SEM. All data were analyzed by linear mixed models followed by comparisons of least square means. Statistical tests were performed in R.

Results

Genetic Inactivation of Slc38a1 Abolishes Interneuron-Like Localization

In order to examine the potential involvement of Slc38a1 in GABA replenishment and synaptic plasticity *in vivo*, we used the binary Cre/LoxP system to genetically inactivate Slc38a1 in mice by deleting exons 5–8 (Fig. 1A). Genetic identity was confirmed by PCR using 3 pairs of primers and by Southern blotting (Fig. 1B–C). The genotypes were further corroborated by analyses of RNA transcripts (not shown) and Slc38a1 protein expression by Western blotting showing no expression of the protein in Slc38a1$^{-/-}$ mice (Fig. 1D). In brain, overall cell numbers and cortical cytoarchitecture were identical in both genotypes (Fig. S1A–F). Immunoperoxidase staining for Slc38a1 accumulates in scattered interneuron-like cells in Slc38a1$^{+/+}$ mice while it is entirely abolished in brain sections from Slc38a1$^{-/-}$ mice (Fig. 1E, S1G–J). Thus, DNA, RNA and protein analyses confirm successful inactivation of Slc38a1 in mice, and exclude major phenotypic abnormalities for brain anatomy. Moreover, these data points to Slc38a1 as specific for neurons with interneuron-like layer distribution.

Slc38a1 Inactivation Alters Levels of Key AAs and Enzymes Involved in GABA Synthesis

We next investigated the functional significance of Slc38a1-mediated glutamine transport for the metabolic and/or neurotransmitter pools of several AAs. Analyses of forebrain extracts obtained from Slc38a1$^{+/+}$ and Slc38a1$^{-/-}$ mice show significantly reduced levels of AAs associated with the GABA metabolism and the GGG cycle, i.e., glutamine, glutamate, GABA and aspartate (Fig. 2A). In contrast, other AAs, such as alanine, serine, glycine, and taurine, remained unchanged upon Slc38a1 inactivation (Fig. 2A). These data implicate a role for Slc38a1 in the replenishment of AAs potentially involved in GABAergic neurotransmission *in vivo*.

Next, we assessed whether the reduced pools of AAs represented metabolic intermediates or neurotransmitters by analyzing synaptosomal fractions from Slc38a1$^{+/+}$ and Slc38a1$^{-/-}$ mice for AA content. Synaptosomes are suitable for first assessment of specialized neurotransmitter pools (Biesemann et al. 2014; Hassel et al. 2015) although they are contaminated with gliosomes. We detected a significant reduction in synaptosomal glutamine and aspartate levels (Fig. 2B), the latter is formed downstream of GABA. In contrast, the GABA-homolog taurine—an osmolyte that does not participate in GABA metabolism or the GGG cycle—remains unchanged upon Slc38a1 inactivation (Fig. 2B).

As synaptosomal GABA levels are sub-significantly reduced, we hypothesized that Slc38a1 disruption activates compensatory mechanisms to maintain GABAergic neurotransmission. We therefore quantified key proteins involved in glutamate and GABA metabolism and signaling. Relative to wild-type (wt) littermates, Slc38a1$^{-/-}$ mice showed significantly higher levels of
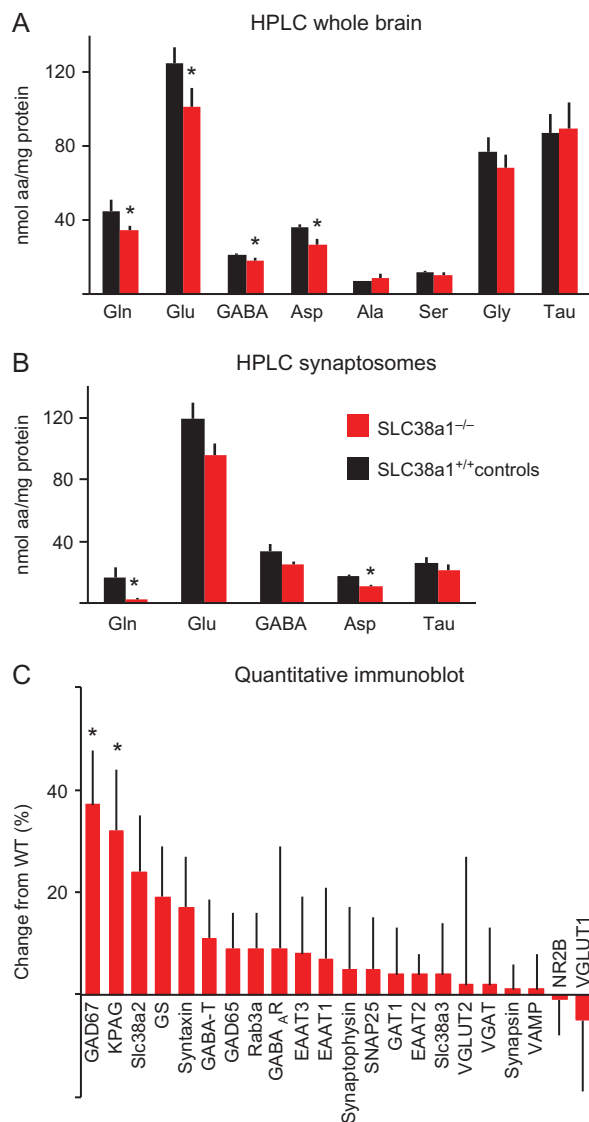
Figure 2. Slc38a1 inactivation reduces selectively levels of amino acids (AA) and increases levels of proteins sustaining GABA transmission. (A) The concentration of AAs in forebrains of Slc38a1$^{-/-}$ (red) and Slc38a1$^{+/+}$ (black) mice (n = 5 in each group) were investigated by HPLC. Significant reduction in the levels of glutamine (Gln), glutamate (Glu), GABA and aspartate (Asp) was detected upon Slc38a1 inactivation. The levels of some other AAs, such as alanine (Ala), serine (Ser), glycine (Gly) or taurine (Tau), were not altered. (B) Synaptosomes were made from brains of Slc38a1$^{-/-}$ (red) and Slc38a1$^{+/+}$ (black) mice and their content of AAs was measured by HPLC: Glutamine and aspartate are significantly reduced. Glutamate and GABA are sub-significantly reduced, while there is no difference in the concentrations of taurine in Slc38a1$^{-/-}$ compared to Slc38a1$^{+/+}$. (C) Quantitative immunoblotting of total brain extracts from Slc38a1$^{-/-}$ and Slc38a1$^{+/+}$ mice shows significant up-regulation of GAD67 and PAG in Slc38a1$^{-/-}$ mice compared to Slc38a1$^{+/+}$ mice. Proteins associated with glutamatergic neurotransmission, such as NR2B and VGLUT1, are not increased. GAD67, Glutamic acid decarboxylate (GAD) 67 kDa; PAG, (kidney) Phosphate-activated glutaminase; Slc38a2, Slc38 family member 2: The System A transporter 2 (SAT2/SNAT2); GS, Glutamine synthetase; GABA-T, GABA aminotransferase; GAD65, GAD 65 kDa; Rab3a, The RAS-related protein 3 A; GABA$_A$R, GABA$_A$ receptor; EAAT3, Excitatory amino acid transporter (EAAT) 3 (Slc1a1); EAAT1 (Slc1a3); SNAP25, Synaptosomal-associated protein 25; GAT1, GABA transporter 1 (Slc6a1); EAAT2 (Slc1a2); Slc38a3, Slc38 family member 3: The System N transporter 1 (SN1/SNAT3); VGLUT2, Vesicular glutamate transporter (VGLUT) 2 (Slc17a6); VGAT, Vesicular GABA transporter (Slc32); VAMP, Vesicle-associated membrane protein; NR2B, NR2B subunit of NMDA receptor; VGLUT1 (Slc17a7). Red and black bars in A and B: Slx38a1$^{-/-}$ and Slx38a1$^{+/+}$, respectively. Data are mean ± SD values. Asterisk: different from control; P < 0.007 (A,C: unpaired Student's t-test, B: Mann–Whitney test).

GAD67, the enzyme catalyzing glutamate to GABA conversion (Fig. 2C). Likewise, the upstream enzyme, PAG, catalyzing glutamine to glutamate conversion, is up-regulated in Slc38a1$^{-/-}$ mice (Fig. 2C). This suggests that GABA formation is distorted and that 2 key enzymes in the GABA synthesis pathway are up-regulated to overcome metabolic restrictions to maintain GABA (and its precursor glutamate) in nerve terminals. Expression of proteins contributing to the vesicular sequestration of GABA or glutamate, their receptors or plasma membrane transporters, remained unchanged. Altogether, our data suggest a selective role for Slc38a1 in GABA replenishment in harmony with its localization in interneurons (Fig. 1E, S1G–J).
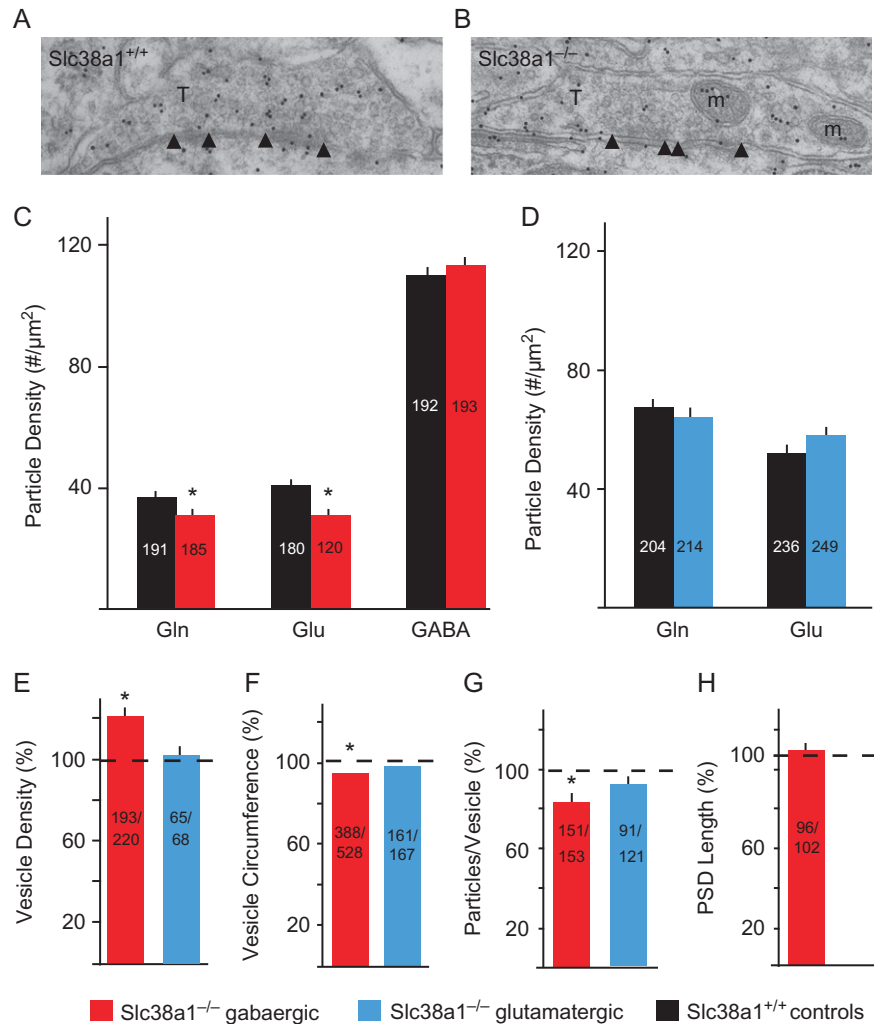
Slc38a1 Deletion Alters Vesicle Morphology and Reduces Vesicular GABA Content

In order to reveal the impact of Slc38a1 on vesicular neurotransmitter content and synaptic transmission, we next studied synapse morphology and concentrations of the 2 main fast neurotransmitters and their putative precursor by electron microscopy. In the hippocampus, the number and morphological appearance of synapses, as well as subcellular structures were unchanged between Slc38a1$^{+/+}$ and Slc38a1$^{-/-}$ mice (Fig. 3A and B, S2A). Immunogold labeling of inhibitory nerve terminals (which represents the total vesicular and extra-vesicular concentration of the amino acids) of the hippocampal CA1 demonstrated significant reduction of glutamine and glutamate while GABA levels were sustained (Fig. 3A–C). This is congruous with a shift in the equilibrium to form GABA at the expense of its 2 precursors, glutamine and glutamate, and is consistent with our synaptosomal HPLC data and upregulated PAG and GAD67 expressions (Fig. 2). The selective role of Slc38a1 in GABAergic neurotransmitter replenishment is corroborated by a lack of any influence in adjacent glutamatergic nerve terminals since both glutamine and glutamate concentrations are preserved in Slc38a1$^{-/-}$ mice (Fig. 3D).

We then specifically focused on synaptic vesicles: the relative distribution of synaptic vesicles from the release site remains intact in Slc38a1$^{-/-}$ mice (Fig. S2B). However, the density of synaptic vesicles in Slc38a1$^{-/-}$ GABAergic terminals is increased (Fig. 3E; ~21% augmentation). In addition, there is a small, but significant reduction (in the circumference of GABAergic synaptic vesicles (Fig. 3F; ~8% reduction in volume). This is corroborated by immunogold labeling for GABA showing reduced vesicular content (Fig. 3G; ~16% GABA reduction). However, Slc38a1 inactivation was not associated with any significant change in the length of the post-synaptic density at GABAergic synapses (Fig. 3H) suggesting that Slc38a1$^{-/-}$ synapses retain GABA signaling at near-physiological levels. Interestingly, Slc38a1 deletion has no impact on vesicle density, vesicle circumference or vesicular neurotransmitter content in glutamatergic nerve terminals (Fig. 3E–G) corroborating a selective impact on GABAergic neurotransmission. Thus, Slc38a1 disruption significantly reduces the specific vesicular GABA content.

Slc38a1$^{-/-}$ Mice Retain Normal Excitatory Synaptic Transmission and Synaptic Plasticity

To investigate any functional role for Slc38a1 in excitatory synaptic transmission and synaptic excitability, simultaneous electrophysiological recordings were conducted in the apical dendritic and soma layers in the CA1 region of hippocampal slices from Slc38a1$^{-/-}$ and Slc38a1$^{+/+}$ mice. We found no substantial differences in fiber density, number of afferent fibers,

Figure 3. Slc38a1 inactivation alters synaptic vesicle morphology and GABAergic vesicular load. Pieces of hippocampal CA1 from Slc38a1$^{+/+}$ and Slc38a1$^{-/-}$ mice were dissected out, embedded in resins and examined by immunogold electron microscopy. (A–B) Two electron micrographs (from Slc38a1$^{+/+}$ and Slc38a1$^{-/-}$ mice, respectively) showing putative GABAergic nerve terminals making symmetric synapses onto pyramidal cell dendrites and stained for glutamine. Arrow heads demark synapses. (C) In GABAergic nerve terminals of the stratum radiatum, the immunoreactivities for glutamine and glutamate are significantly reduced while GABA levels are sustained in Slc38a1$^{-/-}$ mice compared to Slc38a1$^{+/+}$ mice. (D) Immunoreactivities for glutamine or glutamate in neighboring glutamatergic nerve terminals are not reduced upon deletion of Slc38a1. (E) The density of synaptic vesicles in putative GABAergic nerve terminals is increased in Slc38a1$^{-/-}$ mice compared to Slc38a1$^{+/+}$ mice. Such change in synaptic vesicle density is not seen in adjacent glutamatergic nerve terminals. (F) The circumference of synaptic vesicles in GABAergic and glutamatergic nerve terminals was measured. GABA$^+$ synaptic vesicles had a small but significant reduction in the circumference in Slc38a1$^{-/-}$ mice. The circumference of synaptic vesicles in glutamatergic nerve terminals withstood any changes upon genetic inactivation of Slc38a1. (G) The vesicular concentration of GABA and glutamate was assessed by measuring immunogold labeling of synaptic vesicles. Vesicular GABA is reduced in Slc38a1 knock-out mice compared to the wild type mice. No significant changes were detected for the vesicular glutamate concentration. (H) There is no significant change in the size of the postsynaptic density (PSD) at GABAergic synapses in Slc38a1$^{-/-}$ mice compared to Slc38a1$^{+/+}$ mice. Structures or staining related to GABAergic or glutamatergic synapses are shown in red and blue, respectively, while the black bars represent the corresponding structures or staining in wt mice. The numbers written on the bars indicate the number of structures analyzed. In E-H the percentage ratio between data obtained in Slc38a1$^{-/-}$ and Slc38a1$^{+/+}$ are shown. m, miotchondria; T, terminal. Asterisk: different from control; $P < 0.007$, unpaired Student's t-test.

amount of excitatory synaptic transmission or excitability (Fig. 4A–C). Thus, these results do not support any major changes in either excitatory synaptic transmission or in postsynaptic excitability when tested by synaptic activation, and reconcile well with our electron microscopy data on glutamatergic synapses. A comparison of paired-pulse facilitation, a short-lasting form of synaptic plasticity primarily attributed to changes in presynaptic Ca^{2+} homeostasis (Zucker and Regehr 2002), reveals no significant difference between the 2 genotypes (Fig. 4D). Finally, prolonged activation (20 Hz 50 s) of afferent fibers in the CA3-to-CA1 pathway or examination of LTP at hippocampal CA3-to-CA1 synapses in slices taken from adult mice

showed no differences between the 2 genotypes (Fig. 4E–G). Altogether, our data do not show any major impact of Slc38a1 inactivation on glutamatergic synaptic transmission (See SI for detailed results).

Glutamine Discharges Perisomatic Interneurons

As Slc38a1 is preferentially expressed by hippocampal and cortical parvalbumin (PV)$^+$ interneurons (also termed fast-spiking (FS) cells; Fig. 5A), we hypothesized that particularly efficacious means of GABA replenishment might have evolved to drive AP firing at high frequencies. Here, we pharmacologically probe
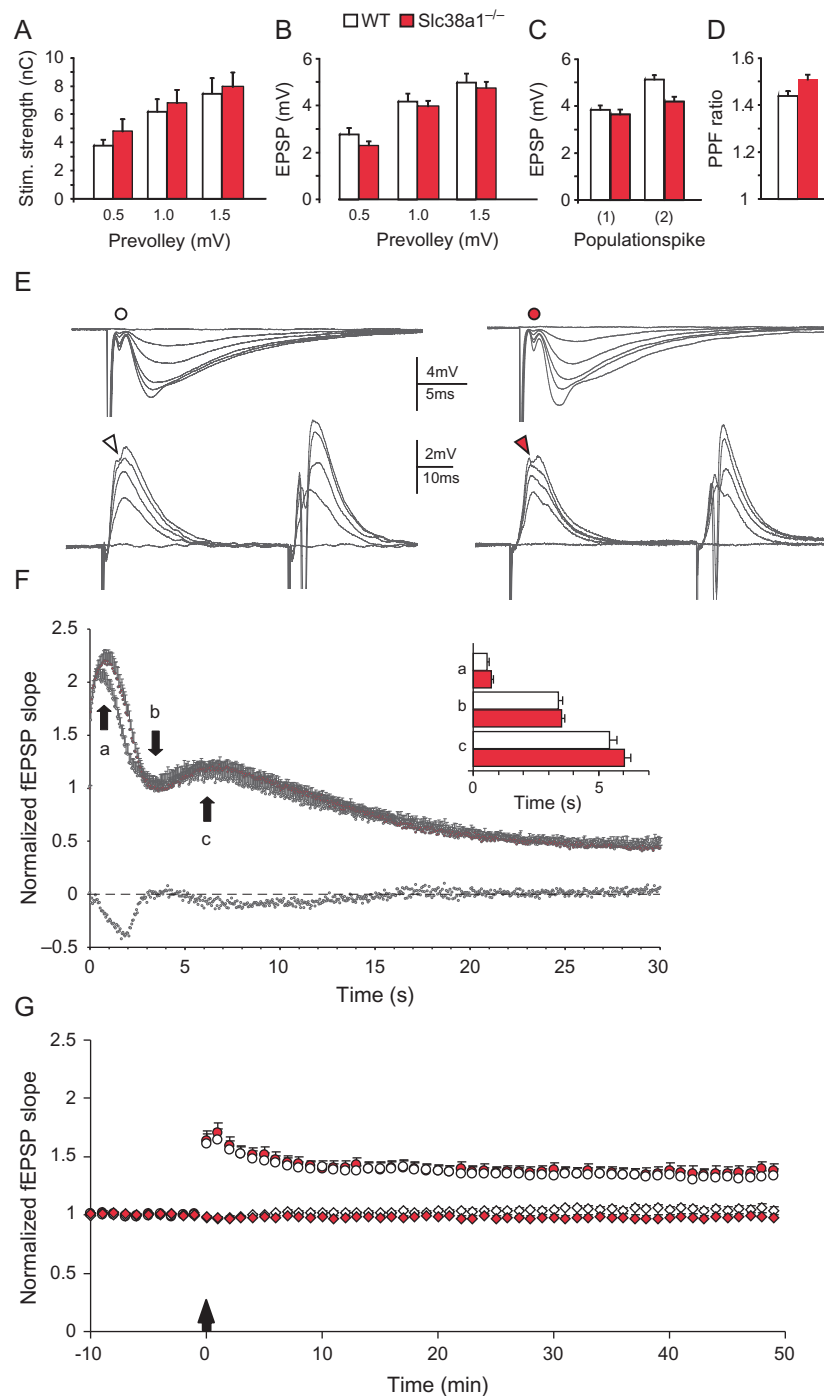
Figure 4. Normal hippocampal excitatory transmission and synaptic plasticity prevail in Slc38a1$^{-/-}$ mice. Excitatory transmission and short- and long-term synaptic plasticity were investigated at hippocampal CA3-to-CA1 synapses. (A) There are no changes in stimulation strengths necessary to elicit a fiber volley of given amplitudes (0.5, 1.0 and 1.5 mV) in Slc38a1$^{-/-}$ mice compared to wild type mice suggesting no difference in fiber density/number of afferents. (B) Field excitatory post-synaptic potential (fEPSP) amplitudes as a function of the same 3 fiber volley amplitudes are equal in the 2 genotypes suggesting normal excitatory synaptic transmission. (C) The fEPSP amplitudes necessary to elicit a just detectable population spike (1) and a population spike of 2 mV (2) are not altered suggesting no impact on pyramidal cell excitability. (D) No significant changes were detected in the paired-pulse facilitation (PPF) ratio in the 2 genotypes at an interstimulus interval of 50 ms. (E) Top row; each trace is the mean of 5 consecutive synaptic responses in stratum radiatum elicited by different stimulation strengths in slices from Slc38a1$^{+/+}$ (left) and Slc38a1$^{-/-}$ (right) mice. The prevolleys preceding the fEPSPs are indicated by circles. Bottom row; recordings from stratum pyramidale elicited by paired-pulse stimulation (50 ms interstimulus interval). Arrowheads indicate the population spike thresholds. (F) Normalized and pooled fEPSP slope measurements during the initial 30 seconds of 20 Hz stimulation in stratum radiatum in slices from Slc38a1$^{+/+}$ and Slc38a1$^{-/-}$ mice. Vertical bars indicate S.E.M. Subtractions of the values obtained in Slc38a1$^{+/+}$ mice from those obtained in Slc38a1$^{-/-}$ mice are represented by the black, open symbols. The inset graph shows *a* the time point of the maximum magnitude of the initial frequency facilitation (as indicated by an arrow in the figure), *b* time point to the transition point between the initial frequency facilitation and the delayed response enhancement (DRE), *c* time needed to reach the peak of the DRE. (G) Normalized, pooled and superimposed extracellular fEPSP slopes evoked at CA3–to-CA1 synapses in slices from Slc38a1$^{+/+}$ and Slc38a1$^{-/-}$ mice. Tetanized pathways are shown with circles and untetanized control pathways are shown with squares. Arrowhead indicates time point of tetanic stimulation. D, F and G suggest no major differences between the genotypes in some forms of short-term and long-term synaptic plasticity. Data are shown as mean ± standard error of mean (S.E.M). Experiments are shown with open symbols for Slc38a1$^{+/+}$ mice and red, filled symbols for Slc38a1$^{-/-}$. None of the comparisons between the genotypes were statistically significant (P < 0.05).

Slc38a1-dependent glutamine uptake for GABA production and vesicular filling and correlate this with neuronal AP patterns. Besides *ex vivo* slice recordings, we developed a culture protocol to specifically enrich and maintain FS cells (Berghuis et al. 2004). We also used irregular-spiking (IR-like) interneurons with discharge frequencies <50 Hz as controls.

Glutamine uptake through SATs was previously reported to depolarize interneurons and to induce paired-pulse facilitation at inhibitory synapses in the hippocampus (Chaudhry et al. 2002). Here, we first reproduced these findings by applying 5 mM glutamine (for lower concentrations, *data not shown*) that depolarized PV$^+$ cortical interneurons (Fig. 5A–B). Glutamine transport through SATs relies on Na$^+$ co-transport with maximal transporter efficacy at resting membrane potentials in the presence of high Na$^+$ concentrations (Chaudhry et al. 2002). Indeed, membrane depolarization was driven by an inward Na$^+$ current with its reversal potential closely matching the calculated Na$^+$ reversal potential (0 mV) when using 20 mM KCl intracellularly (Fig. 5C). Moreover, glutamine transport in FS cells showed significant outward rectification at <−50 mV as opposed to a linear *I-V* relationship seen in control (Fig. 5C; S3B) and upon washout (*data not shown*) in the presence of 125 mM extracellular Na$^+$ and pharmacologically-muted synaptic neurotransmission. Input resistance did not change during glutamine-induced depolarization, suggesting gating by intra-membrane proteins without "*on-demand*" membrane insertion, and reversed upon wash-out (Fig. S3A). These data suggest that glutamine undergoes Na$^+$-dependent electrogenic transport in FS cells through a mechanism operating well at deep resting membrane potentials, which corroborates data on transporter kinetics when Slc38a1 was expressed heterologously in Xenopus oocytes (Chaudhry et al. 2002).

Previously, glutamine-induced depolarization was estimated as ≤ 5 mV (Chaudhry et al. 2002) when measured at low temporal resolution. We reproduced these records at high sampling rates and using methyl aminoisobutyric acid (MeAIB) as SAT substrate to show an incremental (±3 mV) depolarization (Fig. 5D). However, when co-applying glutamine, we found a rapid membrane shift towards −40 mV (AP threshold for cultured FS cells (Berghuis et al. 2004), above which repetitive membrane oscillations with frequencies ranging from 1.8 to 2.5 Hz occurred (Fig. 5D). Glutamine-induced oscillations overshot 0 mV, thus qualifying as AP trains, and were long-lasting yet tended to decrease in frequency (Fig. 5D, end of trace). We attributed their gradual decline to metabolic strain on the neurons we probed. Moreover, both MeAIB and glutamine markedly increased the amplitude of spontaneous inhibitory postsynaptic currents (sIPSCs; 145.9 ± 9.8% and 180.3 ± 13.2% of the baseline, respectively; Fig. S3C) when measured in FS cells receiving significant recurrent inhibitory input from other FS cells in hippocampal CA1 (Galarreta and Hestrin 1999). Thus, glutamine uptake through Slc38a1 might reset network excitability by driving FS cell activity.

We then exploited interneuron-enriched cultures (Berghuis et al. 2004) to dissect the electrogenic signature of glutamine uptake. In FS-like cells, which expressed Slc38a1 perisomatically as well as in processes (Fig. 5E, E_1), current-clamp recordings showed that increasing the glutamine concentration from 2 to 5 mM extracellularly evoked robust depolarization ($P < 0.05$ at 3 and 6 min *vs.* IR controls, $n = 7/12$; Fig. 5F). Discharge events were highly ordered, their frequency increased with ongoing glutamine superfusion (Fig. 5G), and reached steady-state by ~5 min of glutamine application when the raid surge in membrane potential is followed by a 1–2 s depolarization state and a subsequent rapid repolarization step (Fig. 5G_1, *panel c*). Upon glutamine wash-out, both the frequency and amplitude of membrane depolarization gradually subsided. Pre-treatment with 100 µM 3-Mercaptopropionic acid (3-MPA), a GAD inhibitor, abolished glutamine-induced depolarization, suggesting end-point (product) regulation (Fig. 5F). These events were insensitive to AMPA, kainate or mGluR antagonists, excluding bias by glutamine-to-glutamate conversion (Fig. S3D, D_1). Moreover, glutamine primes this phenomenon since step-wise depolarization fails to evoke any similar discharge (Fig. S3E). Notably, glutamine-induced changes were observed in FS-like but less so in IR-like cells (Fig. 5F), which is consistent with IR-like cells expressing alternative transport systems. Collectively, we suggest that glutamine can tonically excite FS interneurons, at least in isolation.

Deletion of Slc38a1 Alters Gamma Oscillations In vivo

Given that pharmacological probing of Slc38a1 alters interneuron activity and that maturation of PV$^+$ FS neurons dictates onset of the enhanced plasticity period in early postnatal life (Hensch 2005), we next investigated if cortical processing and plasticity were also altered in the Slc38a1$^{-/-}$ *in vivo*. Extracellular recordings of single unit activity and local field potentials (LFP) from the primary visual cortex of anesthetised Slc38a1$^{-/-}$ mice at the peak of the critical period (P29-31) revealed that oscillations in the gamma (ɣ) frequency band (30–90 Hz) were significantly slower compared to Slc38a1$^{+/+}$ (Fig. 6A–B). Gamma activity is thought to be important for cognition and arises from synchronous activity of FS PV$^+$ interneurons (Buzsaki and Wang 2012). The slower ɣ frequency of the Slc38a1$^{-/-}$ resembles what has been found in immature PV$^+$ network where there is also lower levels of GABA and which is characteristic of pre- critical period conditions (Hensch 2005; Ben-Ari et al. 2007).

Deletion of Slc38a1 Alters the Activity of Visual Cortex Inhibitory Neurons

To examine if Slc38a1 deletion affects neuronal activity on the single-cell level we recorded 282 single units from the primary visual cortex (109 units from Slc38a1$^{-/-}$ ($N = 11$) and 173 from Slc38a1$^{+/+}$ ($N = 11$)). Recorded units were classified as putatively excitatory (broad-spiking) or inhibitory (narrow-spiking) neurons based on spike waveform parameters (Bartho et al. 2004) (Fig. 6C–D, S4A).

Both genotypes responded to visual stimuli (drifting gratings) (Fig. 6E), and firing rates of excitatory units were comparable between Slc38a1$^{-/-}$ and Slc38a1$^{+/+}$ (Slc38a1$^{-/-}$: 1.7 ± 04 spikes/s versus Slc38a1$^{+/+}$: 2.1 ± 0.4 spikes/s; Fig. 6F). In contrast, spontaneous activity of inhibitory units recorded in Slc38a1$^{-/-}$ mice was significantly higher than that of Slc38a1$^{+/+}$ (Slc38a1$^{-/-}$: 3.1 ± 0.9 spikes/s versus Slc38a1$^{+/+}$: 1.5 ± 0.4 spikes/s, generalized linear model, pgenotype:unit type = 0.04, comparisons of least square means, inhibitory units: Slc38a1$^{-/-}$ vs. Slc38a1$^{+/+}$: $P = 0.009$); Fig. 6F), while stimulus-evoked rates did not differ (Fig. S5D). The selective effect of Slc38a1 deletion on baseline activity of inhibitory neurons is consistent with impaired GABAergic neurotransmission and perturbed discharges in FS PV$^+$ interneurons.

Visual cortex neurons respond with preference to stimuli consisting of high contrast lines of specific orientations. Response strength to the preferred orientation measured as orientation selectivity index (OSI) was not affected by Slc38a1
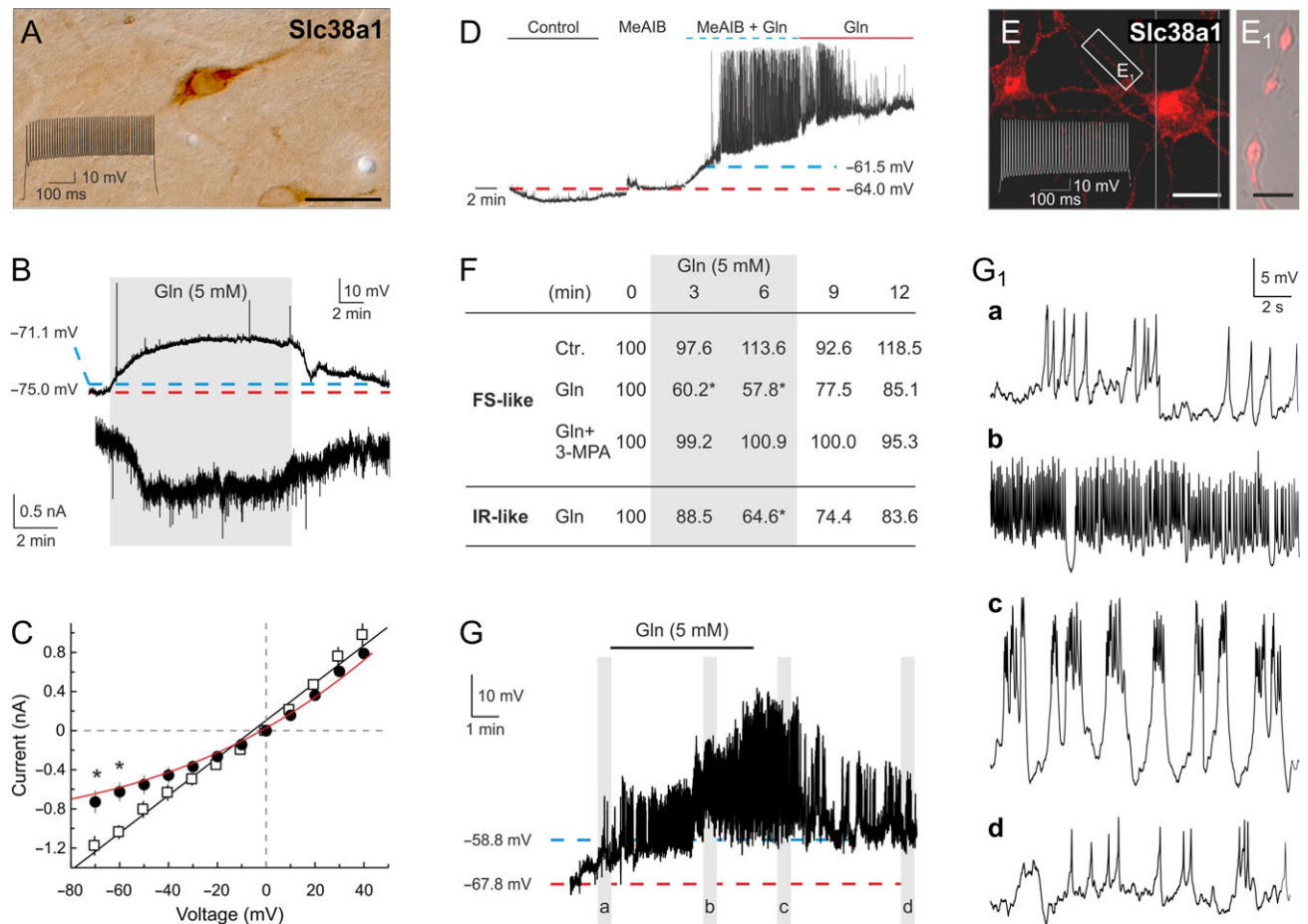
Figure 5. Glutamine induces high-frequency membrane oscillations in neocortical and hippocampal fast-spiking (FS) cells. (A) FS cells in CA1 stratum radiatum express the system A transporter Slc38a1. (B) Glutamine induces membrane depolarization of FS interneurons (*upper panel*) and generates an inward current (*bottom panel*; clamped at −70 mV), which are reversed upon wash-out. Red and blue dashed lines indicate resting membrane potentials at the start and end of current clamp recordings, respectively. (C) Current – voltage relationship of SAT-mediated currents. Open squares refer to superfusion in control, while filled circles in the presence of glutamine (6 min). Note the glutamine-induced outward rectification. *$p < 0.05$ vs. control (Student's t-test, $n = 6$). The reversal potential, conferring to the cross at the abscissa, did not change. (D) Representative current clamp record shows membrane potential oscillations induced by MeAIB and glutamine. Note that glutamine but not MeAIB alone depolarizes the recorded cell. E) Cultured FS-like cells were Slc38a1 immunoreactive at 12 days *in vitro*. Note Slc38a1 localization to varicose axon segments (E_1). *Scale bars* = 30 μm (E), 4 μm (E_1). (F) Glutamine-induced membrane potential depolarization is rapid in FS-like but less so in IR-like interneurons. 3-Mercaptopropionic acid (3-MPA) occludes this response. *$P < 0.05$ *vs.* baseline at 0 min (Student's t-test). gray area denotes the 6-min period of glutamine superfusion. 3-MPA was applied for 16 h at 100 μM concentration. Data were expressed as means from $n = 12$–15 cells/condition. (G) Glutamine elicited a progressive increase in the frequency of membrane oscillations, which can transiently exceed 0 mV after glutamine application for 6 min with gradual repolarization upon wash-out. Vertical gray bars indicate the positions of high-resolution panels (a-d) in G_1. Note the highly conserved time constant and amplitude of unitary Slc38a1-mediated conductance changes.

deletion in neither excitatory nor inhibitory units (Fig. S4B–C), suggesting that the Slc38a1 deletion does not influence basic responses to sensory stimulation.

Slc38a1 Deletion Impairs Ocular Dominance Plasticity

Altered inhibitory neuron activity of Slc38a1$^{-/-}$ resembles that of an immature neural network and could contribute to impaired cortical plasticity. To test this, we used the classical model of ocular dominance plasticity in the primary visual cortex (Levelt and Hubener 2012). The majority of neurons in the binocular part of the primary visual cortex respond stronger to stimulation of the contralateral eye than the ipsilateral eye, a phenomenon called ocular dominance. If the dominant eye is deprived of adequate sensory input during the critical period, the population of binocular neurons will shift their preference towards the non-deprived eye (Hubel et al. 1977). As deletion of Slc38a1 impairs GABAergic function, we posited that ocular

dominance plasticity during the critical period is affected in Slc38a1$^{-/-}$ mice. Activity-dependent plasticity was experimentally induced by MD for 4 days during the critical period. MD caused a shift in eye preference for excitatory units from the contralateral (deprived) towards the ipsilateral (non-deprived) eye, measured as a reduction in contralateral bias, but the shift was only significant for Slc38a1$^{+/+}$ animals (Fig. 7A–C). Conversely, inhibitory neurons from Slc38a1$^{+/+}$ displayed a shift towards preference for the contralateral (deprived) eye after MD, something which was not seen in Slc38a1$^{-/-}$ animals (Fig. 7D–F).

MD significantly reduced the spontaneous firing rates of both Slc38a1$^{-/-}$ and Slc38a1$^{+/+}$ inhibitory neurons (Fig. S5). Despite their reduced activity, Slc38a1$^{-/-}$ inhibitory units still showed higher spontaneous activity than Slc38a1$^{+/+}$ after MD (S5C). Absence of a normal MD response in Slc38a1$^{-/-}$ animals and the apparent reduction in stimulus-evoked rate of excitatory units after MD (Fig. S5B), resemble pre-critical period conditions (Smith and Trachtenberg 2007). This suggests that
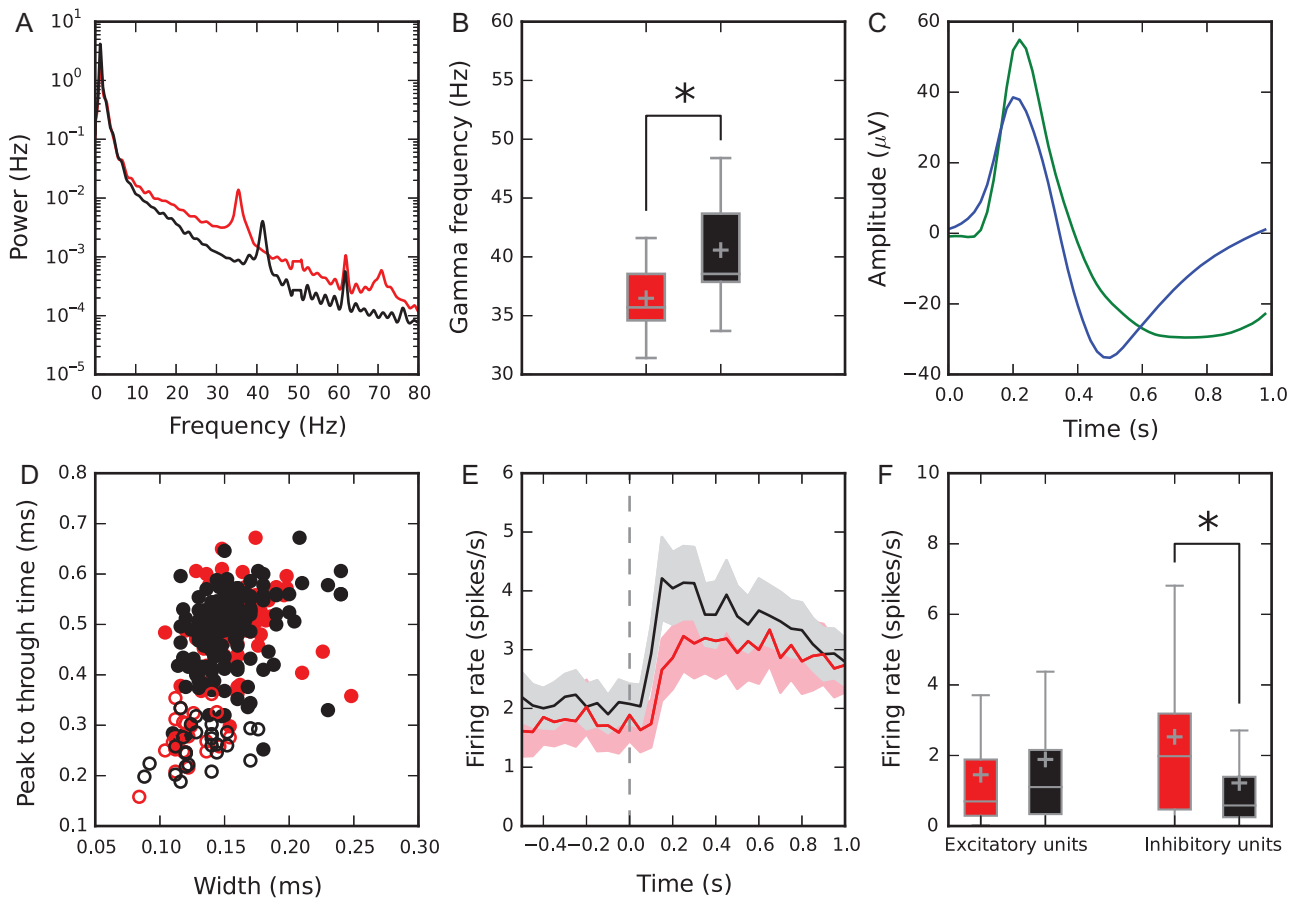
Figure 6. Slc38a1 inactivation alters population activity *in vivo*. (A) Examples of power spectra of LFP in Slc38a1$^{-/-}$ (red) compared to Slc38a1$^{+/+}$ control (black). The peak in the power spectrum of the local field potential was identified in the gamma range (30–90 Hz). (B) Gamma peak frequency was significantly lower in slc38a1$^{-/-}$ mice (n = 10) compared to controls (n = 11) (Slc38a1$^{-/-}$: 37 ± 1 Hz, wt: 44 ± 1 Hz,. Linear mixed model, *$p_{genotype}$ = 0.03). (C) Example waveforms of a broad-spiking puta-tive excitatory unit (green) and narrow-spiking putative inhibitory unit (blue) (D) Spike waveform width plotted against peak-to-trough time for all units (n = 273) showing separate clustering of inhibitory units and excitatory units (filled circles: excitatory units; open circles: inhibitory units). Units were classified based on princi-pal component analysis of waveform parameters. (E) Peristimulus histogram showing average firing rate of putative excitatory neurons in response to visual stimuli of both eyes. Stimulus onset at time 0 (gray line). (F) No difference in spontaneous firing rates of excitatory neurons between the genotypes (Slc38a1$^{-/-}$: 1.7 ± 0.4 spikes/s versus Slc38a1$^{+/+}$: 2.1 ± 0.4 spikes/s). The spontaneous activity of inhibitory units recorded from Slc38a1$^{-/-}$ mice is significantly higher than that of Slc38a1$^{+/+}$ (Slc38a1$^{-/-}$: 3.1 ± 0.9 spikes/s versus Slc38a1$^{+/+}$: 1.5 ± 0.4 spikes/s, generalized linear model, pgenotype:unit type = 0.04, comparisons of least square means, inhibitory units: Slc38a1$^{-/-}$ vs. Slc38a1$^{+/+}$: P = 0.009).

deletion of Slc38a1 may contribute to render the cortical net-work in an immature state; unable to enter the critical period due to impaired GABA signaling. In this respect, Slc38a1 appears to be of fundamental importance for normal cortical development and GABA-dependent plasticity.

Discussion

We establish that Slc38a1 is enriched in PV$^+$ interneurons and that Slc38a1 disruption has impact on synaptic vesicle size, vesicular load and GABAergic signaling (for summary of the results see Fig. S6). Slc38a1 drives FS cell activity, triggers AP generation and regulates network excitability. Genetic inactivation of Slc38a1 altered ocular dominance plasticity and γ oscillations suggesting impaired GABA signaling resembling neuronal networks in an immature state. Collectively, our data implicate that Slc38a1 contri-butes to normal cortical development and plasticity. Thus, dys-functional glutamine supply and Slc38a1 activity may contribute to neurologic dysfunction such as in epilepsy, autism, schizophrenia and anxiety (Soghomonian and Martin 1998; Lewis et al. 2012).

Slc38a1 Aids Interneurons to Replenish Neurotransmitter Pools of GABA

Slc38a1$^{-/-}$ mice helped us to show that Slc38a1 is intrinsic to glutamine transport into GABAergic neurons to sustain GABA neurotransmitter pools: glutamine and aspartate, upstream and downstream metabolites of GABA, respectively, are selec-tively and significantly reduced in forebrain extracts and syn-aptosomal fractions. The significant reduction in aspartate in brain extracts and synaptosomes is indicative of a reduced influx of glutamine into the tricarboxylic acid (TCA) cycle of GABAergic neurons, leading to a reduced formation of TCA cycle end product, which equilibrates with aspartate. Our data agree with the notion that system A activity being responsible for 87% of neuronal uptake of glutamine (Kanamori and Ross 2006). Furthermore, they corroborate glutamine as a major pre-cursor for transmitter GABA synthesis, consistent with a large number of classical studies (e.g., Paulsen et al. 1988; Sonnewald et al. 2006). Indeed, oral glutamine supplementation increases CNS levels of GABA (Wang et al. 2007).
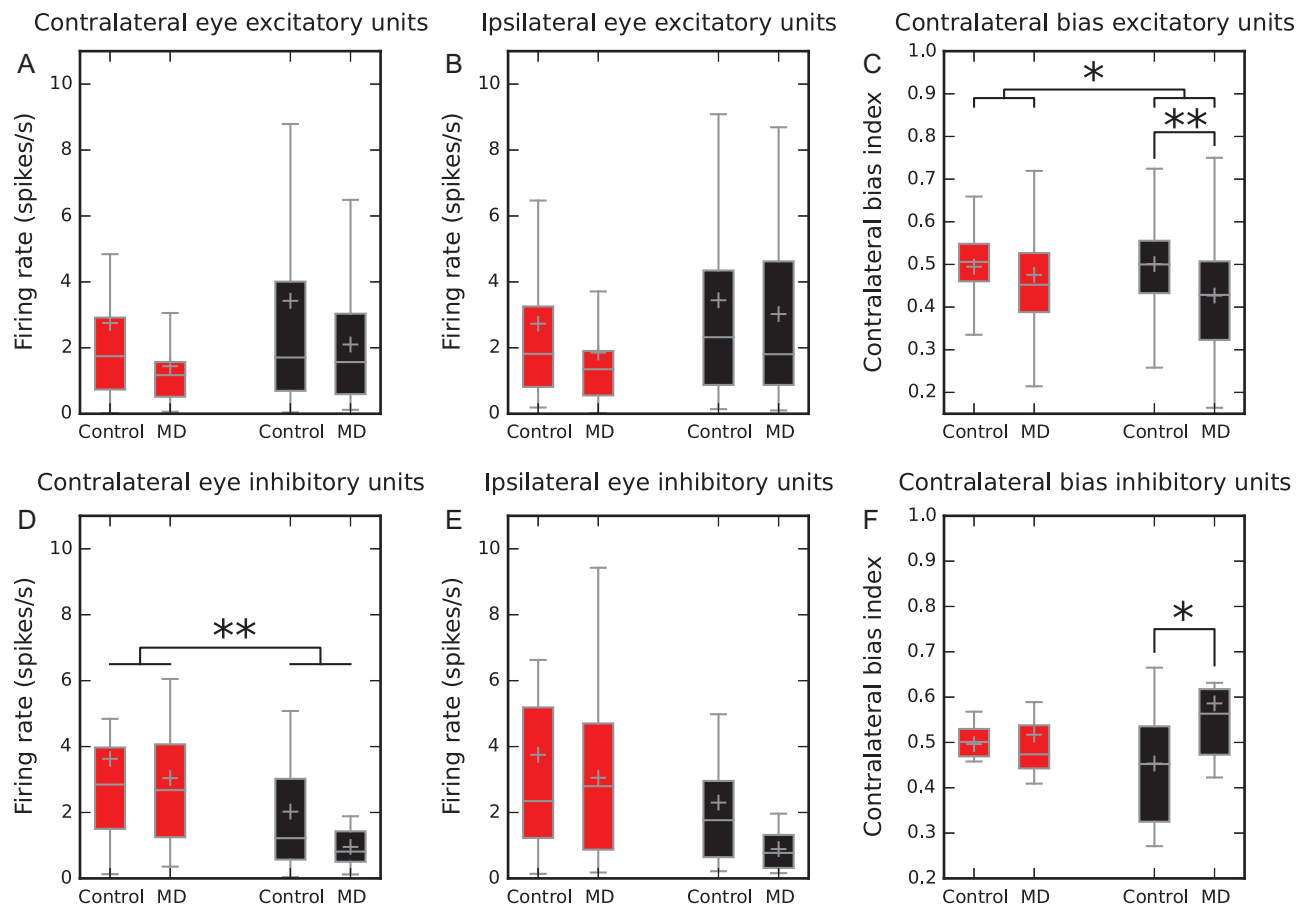
Figure 7. Altered ocular dominance plasticity in Slc38a1$^{-/-}$ mice. Stimulus evoked firing rates of excitatory (A,B) and inhibitory (D,E) units in response to stimulation of contralateral (deprived) and ipsilateral (non-deprived) eyes with drifting gratings for slc38a1$^{-/-}$ (red) and Slc38a1$^{+/+}$ (black) animals exposed to 4 days monocular deprivation (MD) compared to untreated controls. For inhibitory units, Slc38a1$^{-/-}$ had significantly higher contralateral eye evoked rates compared to Slc38a1$^{+/+}$ (linear mixed model, $p_{genotype:unit\ type}$ = 0.002; Comparison of least square means, $p_{IN:\ ko\ vs.\ wt}$ = 0.008). Contralateral bias was calculated based on responses to contralateral vs. ipsilateral eye (C/(C + I)), with higher score indicating greater relative response to contralateral eye. (C) For excitatory units, monocular deprivation led to a shift to lower contralateral bias, however, on group level, this shift was only significant for Slc38a1$^{+/+}$ animals (Slc38a1$^{-/-}$: 0.495 ± 0.02, MD: 0.48 ± 0.02; Slc38a1$^{+/+}$: 0.500 ± 0.012; MD: 0.43 ± 0.02, Linear mixed model, $p_{treatment}$ = 0.04; $p_{genotype:treatment:unit\ type}$ = 0.01; Comparison of least square means: $p_{EX:\ ko\ vs.\ wt}$ = 0.01; $p_{EX,wt:control\ vs.\ MD}$ = 0.004). F) For inhibitory units, monocular deprivation led to a shift towards higher contralateral bias in Slc38a1$^{+/+}$ animals (0.45 ± 0.03, $p_{IN:\ wt:\ Control\ vs.\ wt}$ = 0.02), while no such shift took place in Slc38a1$^{-/-}$ animals (control: Slc38a1$^{-/-}$: 0.50 ± 0.02; Slc38a1$^{+/+}$:; MD: Slc38a1$^{-/-}$: 0.52 ± 0.04; Slc38a1$^{+/+}$: 0.59 ± 0.07, $p_{wt:\ IN:\ control\ vs.\ MD}$ = 0.02).

As the reduction of glutamine and GABA in Slc38a1$^{-/-}$ mice is significant yet they survive and process information properly, we suggest the existence of alternative pathways to maintain a certain level of vesicular GABA. In Slc38a1$^{-/-}$ mice, GAT1 expression is preserved. This suggests that GABA re-uptake into nerve terminals maintains basic GABAergic activity and prevents mal-development and/or mal-function of the brain as described for GAT1$^{-/-}$ mice (Jensen et al. 2003). Key enzymes involved in GABA synthesis from glutamine (GAD67 and PAG) are significantly increased, and the preservation of GABA occurs at the expense of glutamine and glutamate. Tonic non-vesicular release of GABA from GABAergic neurons or astroglial cells, e.g., by the calcium-activated anion channel Bestrophin-1 (Lee and Schwab 2011; Oh and Lee 2017; Soghomonian and Martin 1998) may also contribute to maintain GABAergic activity. Thus, Slc38a1 is intrinsic for GABA formation, with additional mechanisms existing to partly offset the metabolic drain that occurs in Slc38a1 ko animals.

Interestingly, Slc38a1 inactivation upregulates GAD67 but not GAD65. GAD65 is enriched in nerve terminals, functionally couples to VGAT on synaptic vesicle membranes to facilitate the generation and accumulation of GABA inside synaptic vesicles for phasic synaptic release (Jin et al. 2003). In contrast, GAD67 is shown to synthesize most GABA and is involved in generating GABA also for non-vesicular release and tonic firing (Buddhala et al. 2009). Interestingly, GAD67$^{-/-}$ mice have significantly reduced brain GABA concentrations while GABA levels appear normal in GAD65$^{-/-}$ (Soghomonian and Martin 1998). Our data are thus consistent with GAD67 activity being selectively regulated by GABA levels (Soghomonian and Martin 1998).

Slc38a1 Defines GABAergic Vesicular Dynamics and Content

Slc38a1 inactivation impacts synaptic vesicle biology in GABAergic neurons in 3 ways: (1) vesicle size is reduced, (2) vesicular GABA content is reduced, while (3) vesicle density is increased. Interestingly, many pre-synaptic factors have been identified to be involved in defining vesicular content by regulating vesicular filling and/or vesicular recycling (Edwards 2007). The vesicular loading of

e.g., dopamine depends on extracellular concentrations of dopamine and on activation of tyrosine hydroxylase (Pereira and Sulzer 2012). We see reduced cytosolic concentrations of glutamate and glutamine in GABAergic neurons. Our data corroborate that vesicular GABA is in steady state with extra-vesicular glutamate concentration and that Slc38a1-mediated glutamine transport regulates GABAergic quantal size (Mathews and Diamond 2003; Kanamori and Ross 2006). The reduction in vesicle size may be due to reduced transmitter amount and shrunken vesicles, as a linear relationship has been demonstrated between quantal size and vesicular volume (Karunanithi et al. 2002). Finally, the number of synaptic vesicles may have been increased to overcome reduced vesicular content and to sustain GABAergic neurotransmission. Alternatively, a reduction in the vesicular GABA content and dependence relatively more on re-uptake through GAT1 may have increased the pool of releasing vesicles that may be smaller in size (Steinert et al. 2006). Altogether, our data demonstrate that Slc38a1 activity has impact on GABAergic vesicular content.

Deletion of Slc38a1 Alters Cortical Processing and Plasticity *In vivo*

Activity of PV$^+$ interneurons is sufficient to drive γ oscillations (Cardin et al. 2009). Models of immature and mature PV$^+$ inhibitory networks show a development of γ oscillations from low coherence and slower frequency in immature networks towards higher γ frequency oscillations of greater coherence in mature networks, reaching adult levels by the fourth week of life (Doischer et al. 2008). Hence, the lower frequency γ oscillations in Slc38a1$^{-/-}$ mice may reflect immaturity of PV$^+$ inhibitory neurons. The higher firing activity observed in Slc38a1$^{-/-}$ inhibitory neurons is in harmony with a compensation for lower GABA quantal size as inhibitory neurons in general and PV$^+$ neurons in particular have strong self-inhibition (Pfeffer et al. 2013). Such compensation may be insufficient as Slc38a1$^{-/-}$ mice still show slower γ oscillations and altered activity dependent plasticity.

The PV$^+$ inhibitory neurons are established as key players for critical period plasticity. In the visual cortex, this sub-class of inhibitory neurons matures at the time of the critical period and is assumed responsible for opening the period of plasticity. Impaired GABAergic synaptic transmission is therefore likely to affect refinement of cortical circuits. Slc38a1$^{-/-}$ neurons have impaired ocular dominance plasticity in response to MD during the critical period compared to Slc38a1$^{+/+}$ neurons. Our results are similar to those from GAD65$^{-/-}$ mice, where impaired GABA release delays opening of the critical period for ocular dominance plasticity indefinitely (Fagiolini and Hensch 2000), and MD has no discernable effect on ocular dominance of the visual cortex cells. This supports a role for Slc38a1 in GABA-dependent plasticity of the developing cortex.

Conclusions

Slc38a1 is intrinsic for the defining of the GABAergic vesicular load and a key regulator of normal cortical development and presynaptic inhibitory synaptic plasticity. As dysfunctional GABA metabolism and signaling has been associated with several neurological diseases such as in epilepsy, autism, schizophrenia and anxiety (Soghomonian and Martin 1998; Lewis et al. 2012), dysfunctional Slc38a1 activity may play a role in their pathogenesis. Thus, further investigations are required to reveal potential contribution of Slc38a1 to pathophysiology.

Supplementary Material

Supplementary material is available at *Cerebral Cortex* online.

Notes

REFERENCES

Bartho P, Hirase H, Monconduit L, Zugaro M, Harris KD, Buzsaki G. 2004. Characterization of neocortical principal cells and interneurons by network interactions and extracellular features. J Neurophysiol. 92(1):600–608.

Ben-Ari Y, Gaiarsa JL, Tyzio R, Khazipov R. 2007. GABA: a pioneer transmitter that excites immature neurons and generates primitive oscillations. Physiol Rev. 87(4):1215–1284.

Berghuis P, Dobszay MB, Sousa KM, Schulte G, Mager PP, Hartig W, Gorcs TJ, Zilberter Y, Ernfors P, Harkany T. 2004. Brain-derived neurotrophic factor controls functional differentiation and microcircuit formation of selectively isolated fast-spiking GABAergic interneurons. Eur J Neurosci. 20(5):1290–1306.

Biesemann C, Gronborg M, Luquet E, Wichert SP, Bernard V, Bungers SR, Cooper B, Varoqueaux F, Li L, Byrne JA, et al. 2014. Proteomic screening of glutamatergic mouse brain synaptosomes isolated by fluorescence activated sorting. EMBO J. 33(2):157–170.

Bogen IL, Boulland JL, Mariussen E, Wright MS, Fonnum F, Kao HT, Walaas SI. 2006. Absence of synapsin I and II is accompanied by decreases in vesicular transport of specific neurotransmitters. J Neurochem. 96(5):1458–1466.

Boulland JL, Qureshi T, Seal RP, Rafiki A, Gundersen V, Bergersen LH, Fremeau RT Jr., Edwards RH, Storm-Mathisen J, Chaudhry FA. 2004. Expression of the vesicular glutamate transporters during development indicates the widespread corelease of multiple neurotransmitters. J Comp Neurol. 480(3):264–280.

Boulland JL, Rafiki A, Levy LM, Storm-Mathisen J, Chaudhry FA. 2003. Highly differential expression of SN1, a bidirectional glutamine transporter, in astroglia and endothelium in the developing rat brain. Glia. 41(3):260–275.

Brainard GC, Rollag MD, Hanifin JP. 1997. Photic regulation of melatonin in humans: ocular and neural signal transduction. J Biol Rhythms. 12(6):537–546.

Buddhala C, Hsu CC, Wu JY. 2009. A novel mechanism for GABA synthesis and packaging into synaptic vesicles. Neurochem Int. 55(1–3):9–12.

Buzsaki G, Kaila K, Raichle M. 2007. Inhibition and brain work. Neuron. 56(5):771–783.

Buzsaki G, Wang XJ. 2012. Mechanisms of gamma oscillations. Annu Rev Neurosci. 35:203–225.

Cardin JA, Carlen M, Meletis K, Knoblich U, Zhang F, Deisseroth K, Tsai LH, Moore CI. 2009. Driving fast-spiking cells induces gamma rhythm and controls sensory responses. Nature. 459 (7247):663–667.

Chaudhry FA, Reimer RJ, Bellocchio EE, Danbolt NC, Osen KK, Edwards RH, Storm-Mathisen J. 1998. The vesicular GABA transporter, VGAT, localizes to synaptic vesicles in sets of glycingergic as well as GABAergic neurons. J Neurosci. 18(23):9733–9750.

Chaudhry FA, Reimer RJ, Krizaj D, Barber R, Storm-Mathisen J, Copenhagen DR, Edwards RH. 1999. Molecular analysis of System N suggests novel physiological roles in nitrogen metabolism and synaptic transmission. Cell. 99(7): 769–780.

Chaudhry FA, Schmitz D, Reimer RJ, Larsson P, Gray AT, Nicoll R, Kavanaugh M, Edwards RH. 2002. Glutamine uptake by neurons: interaction of protons with system a transporters. J Neurosci. 22(1):62–72.

Conti F, Melone M. 2006. The glutamine commute: lost in the tube? Neurochem Int. 48(6–7):459–464.

Doischer D, Hosp JA, Yanagawa Y, Obata K, Jonas P, Vida I, Bartos M. 2008. Postnatal differentiation of basket cells from slow to fast signaling devices. J Neurosci. 28(48):12956–12968.

Edwards RH. 2007. The neurotransmitter cycle and quantal size. Neuron. 55(6):835–858.

Fagiolini M, Hensch TK. 2000. Inhibitory threshold for critical-period activation in primary visual cortex. Nature. 404(6774):183–186.

Galarreta M, Hestrin S. 1999. A network of fast-spiking cells in the neocortex connected by electrical synapses. Nature. 402 (6757):72–75.

Hamdani eH, Gudbrandsen M, Bjorkmo M, Chaudhry FA. 2012. The system N transporter SN2 doubles as a transmitter precursor furnisher and a potential regulator of NMDA receptors. Glia. 60(11):1671–1683.

Hassel B, Brathe A. 2000. Neuronal pyruvate carboxylation supports formation of transmitter glutamate. J Neurosci. 20(4):1342–1347.

Hassel B, Elsais A, Froland AS, Tauboll E, Gjerstad L, Quan Y, Dingledine R, Rise F. 2015. Uptake and metabolism of fructose by rat neocortical cells in vivo and by isolated nerve terminals in vitro. J Neurochem. 133(4):572–581.

Hensch TK. 2005. Critical period mechanisms in developing visual cortex. Curr Top Dev Biol. 69:215–237.

Hu H, Gan J, Jonas P. 2014. Interneurons. Fast-spiking, parvalbumin(+) GABAergic interneurons: from cellular design to microcircuit function. Science. 345(6196):1255263.

Huang ZJ. 2009. Activity-dependent development of inhibitory synapses and innervation pattern: role of GABA signalling and beyond. J Physiol. 587(Pt 9):1881–1888.

Hubel DH, Wiesel TN, LeVay S. 1977. Plasticity of ocular dominance columns in monkey striate cortex. Philos Trans R Soc Lond B Biol Sci. 278(961):377–409.

Isaacson JS, Scanziani M. 2011. How inhibition shapes cortical activity. Neuron. 72(2):231–243.

Jensen K, Chiu CS, Sokolova I, Lester HA, Mody I. 2003. GABA transporter-1 (GAT1)-deficient mice: differential tonic activation of GABAA versus GABAB receptors in the hippocampus. J Neurophysiol. 90(4):2690–2701.

Jenstad M, Quazi AZ, Zilberter M, Haglerod C, Berghuis P, Saddique N, Goiny M, Buntup D, Davanger S, S Haug FM, et al. 2009. System A transporter SAT2 mediates replenishment of dendritic glutamate pools controlling retrograde signaling by glutamate. Cereb Cortex. 19(5):1092–1106.

Jin H, Wu H, Osterhaus G, Wei J, Davis K, Sha D, Floor E, Hsu CC, Kopke RD, Wu JY. 2003. Demonstration of functional coupling between gamma -aminobutyric acid (GABA) synthesis and vesicular GABA transport into synaptic vesicles. Proc Natl Acad Sci USA. 100(7):4293–4298.

Kam K, Nicoll R. 2007. Excitatory synaptic transmission persists independently of the glutamate-glutamine cycle. J Neurosci. 27(34):9192–9200.

Kanamori K, Ross BD. 2006. Kinetics of glial glutamine efflux and the mechanism of neuronal uptake studied in vivo in mildly hyperammonemic rat brain. J Neurochem. 99(4): 1103–1113.

Karunanithi S, Marin L, Wong K, Atwood HL. 2002. Quantal size and variation determined by vesicle size in normal and mutant Drosophila glutamatergic synapses. J Neurosci. 22 (23):10267–10276.

Klausberger T, Somogyi P. 2008. Neuronal diversity and temporal dynamics: the unity of hippocampal circuit operations. Science. 321(5885):53–57.

Lee M, Schwab C, McGeer PL. Astrocytes are GABAergic cells that modulate microglial activity. Glia 2011;59:152–165.

Levelt CN, Hubener M. 2012. Critical-period plasticity in the visual cortex. Annu Rev Neurosci. 35:309–330.

Lewis DA, Curley AA, Glausier JR, Volk DW. 2012. Cortical parvalbumin interneurons and cognitive dysfunction in schizophrenia. Trends Neurosci. 35(1):57–67.

Liu P, Jenkins NA, Copeland NG. 2003. A highly efficient recombineering-based method for generating conditional knockout mutations. Genome Res. 13(3):476–484.

Mackenzie B, Schafer MK, Erickson JD, Hediger MA, Weihe E, Varoqui H. 2003. Functional properties and cellular distribution of the system A glutamine transporter SNAT1 support specialized roles in central neurons. J Biol Chem. 278(26): 23720–23730.

Masson J, Darmon M, Conjard A, Chuhma N, Ropert N, Thoby-Brisson M, Foutz AS, Parrot S, Miller GM, Jorisch R, et al. 2006. Mice lacking brain/kidney phosphate-activated glutaminase have impaired glutamatergic synaptic transmission, altered breathing, disorganized goal-directed behavior and die shortly after birth. J Neurosci. 26(17):4660–4671.

Mathews GC, Diamond JS. 2003. Neuronal glutamate uptake contributes to GABA synthesis and inhibitory synaptic strength. J Neurosci. 23(6):2040–2048.

Nissen-Meyer LS, Chaudhry FA. 2013. Protein kinase C phosphorylates the system N glutamine transporter SN1 (Slc38a3) and regulates its membrane trafficking and degradation. Front Endocrinol (Lausanne). 4:138.

Nissen-Meyer LS, Popescu MC, Hamdani eH, Chaudhry FA. 2011. Protein kinase C-mediated phosphorylation of a single serine residue on the rat glial glutamine transporter SN1 governs its membrane trafficking. J Neurosci. 31(17):6565–6575.

Oh SJ, Lee CJ. Distribution and Function of the Bestrophin-1 (Best1) Channel in the Brain. Exp Neurobiol. 2017;26: 113–121.

Ottersen OP, Storm-Mathisen J. 1984. Glutamate-and GABA-containing neurons in the mouse and rat brain as demonstrated with a new immunocytochemical technique. J Comp Neurol. 229:374–392.

Paulsen RE, Odden E, Fonnum F. 1988. Importance of glutamine for gamma-aminobutyric acid synthesis in rat neostriatum in vivo. J Neurochem. 13:637–641.

Pereira DB, Sulzer D. 2012. Mechanisms of dopamine quantal size regulation. Front Biosci (Landmark Ed). 17:2740–2767.

Pfeffer CK, Xue M, He M, Huang ZJ, Scanziani M. 2013. Inhibition of inhibition in visual cortex: the logic of connections between molecularly distinct interneurons. Nat Neurosci. 16(8):1068–1076.

Reubi JC, Van Der Berg C, Cuenod M. 1978. Glutamine as precursor for the GABA and glutamate trasmitter pools. Neurosci Lett. 10(1–2):171–174.

Schwenk F, Baron U, Rajewsky K. 1995. A cre-transgenic mouse strain for the ubiquitous deletion of loxP-flanked gene segments including deletion in germ cells. Nucleic Acids Res. 23(24):5080–5081.

Smith SL, Trachtenberg JT. 2007. Experience-dependent binocular competition in the visual cortex begins at eye opening. Nat Neurosci. 10(3):370–375.

Soghomonian JJ, Martin DL. 1998. Two isoforms of glutamate decarboxylase: why? Trends Pharmacol Sci. 19(12): 500–505.

Solbu TT, Bjorkmo M, Berghuis P, Harkany T, Chaudhry FA. 2010. SAT1, A glutamine transporter, is preferentially expressed in GABAergic neurons. Front Neuroanat. 4:1.

Sonnewald U, Kortner TM, Qu H, Olstad E, Sunol C, Bak LK, Schousboe A, Waagepetersen HS. 2006. Demonstration of extensive GABA synthesis in the small population of GAD positive neurons in cerebellar cultures by the use of pharmacological tools. Neurochem Int. 48(6–7):572–578.

Steinert JR, Kuromi H, Hellwig A, Knirr M, Wyatt AW, Kidokoro Y, Schuster CM. 2006. Experience-dependent formation and recruitment of large vesicles from reserve pool. Neuron. 50(5):723–733.

Varoqui H, Zhu H, Yao D, Ming H, Erickson JD. 2000. Cloning and functional identification of a neuronal glutamine transporter. J Biol Chem. 275(6):4049–4054.

Wang L, Maher TJ, Wurtman RJ. 2007. Oral L-glutamine increases GABA levels in striatal tissue and extracellular fluid. FASEB J. 21(4):1227–1232.

Zucker RS, Regehr WG. 2002. Short-term synaptic plasticity. Annu Rev Physiol. 64:355–405.